The Benefit of True Fracture Strain on Material Model Parametrization

Matthias Schneider[1], Matti Teschner[1], Sebastian Westhäuser[1]

[1]Salzgitter Mannesmann Forschung GmbH

1 Abstract

By means of numerical simulation, cars have become much saver and lighter at the same time (when focusing on chassis and body in white). The ongoing improvement of steel grades for the automotive sector has additionally supported this development. Nowadays, the last percentages of improvements can only be obtained by using the latest steel grades and a very realistic modeling of their strain hardening and failure behavior. In case of hot rolled steels with a thickness of 4.0 mm, this leads more and more often to a modeling based on solid finite elements. Focusing hot rolled steels with high yield strength and high formability, there is in addition the need for a modeling of anisotropic hardening.
As presented on the German LS-DYNA users meeting in 2018 [1], the material model ***MAT_TABULATED_JOHNSON_COOK_ORTHO_PLASTICITY** [2, 3] can be parameterized inversely on data from standard tensile tests. Here, the extrapolation of the used hardening curves for 0°, 45° and 90° to rolling direction were determined by an inverse optimization. The target was the minimization of the sums of error squares by comparing the experimental and numerical stress-strain-curves. The comparison with local strain analysis showed an adequate accordance. Unfortunately, when focusing on post-necking strain values, the deviations increased significantly. For future projects, there is a need for a more precise hardening description and an additional failure modeling.
Since the publications of Hance [4] and Larour and Wagner [5], the determination of local ductility measures based on the fracture surface of tensile tests is often discussed. The determination of true fracture strain (TFS) is presently not defined to any standard. In some publications the entire fracture surface [4] (TFS-A) is used for the calculation. In others, only individual sheet thicknesses such as the maximum thinning [6] (TFS-T) are determined. Besides, the use of these results for classifying steel grades with respect to their ductility and the correlation to other experimental results are discussed [7, 8]. In a case study the improvement on hardening and failure modeling by using TFS-data is analyzed.

2 Introduction and Technical Status

The steel grades which are applied to the latest and will be applied to the future cars are more complex than the grades from the last forty years. The numerical modelling of their hardening behavior is quite challenging. Research projects aim for the latest experimental procedures, the most flexible yield loci and hardening approximations. In the last years, the failure modeling with its high complexity was added. Focusing on chassis parts for instance, the thickness to curvature ratio additionally creates a need for the use of solid elements or shell elements with higher complexity. In addition to this aiming for the most realistic modelling, in industrial work, there is also the target of cost reduction. In case of material modelling, the best compromise of modelling quality and effort has to be found at every days work. This leads for instance to some inverse parameterization approaches instead of a time-consuming experimental characterization. Hardening curves can be fitted based on engineering stress-strain curves from tensile tests. This procedure is commonly used for isotropic hardening. In case of an anisotropic hardening, the material model ***MAT_TABULATED_JOHNSON_COOK_ORTHO_PLASTICITY** [2, 3] should be able to be parameterized inversely on data from standard tensile tests in 0°, 45° and 90° to rolling. Additionally, this model is able to deal with a stress-strain curve in thickness direction, which is hard to measure experimentally.
The determination of true fracture strain (TFS) based on the fracture surface of tensile tests is presently not defined to any standard. The entire fracture surface [4] (TFS-A) is used for the calculation as well as the maximum thinning [6] (TFS-T). However, the information about the contour of the fracture surface is a result of anisotropy and anisotropic hardening accumulated until fracture.

3 Motivation and Target of the Study

Many chassis components are made of hot rolled steels with complex hardening behavior. As the anisotropic hardening gets significant beyond uniform elongation, it could be ignored in the past. Having in mind, that safety margins are decreasing in engineering, there is a need of a more realistic modelling without increasing the effort too much.

As a pursued of the work presented at the German LS-DYNA users meeting in 2018 [1] this study shows the improvement on hardening and failure modeling by use of TFS-data. For the study a bainitic hot-rolled steel grade with a thickness of 4.0 mm is used. The stress-strain curves in 0°, 45° and 90° of this steel shows often a crossing at post-necking strains as shown in Fig. 1.

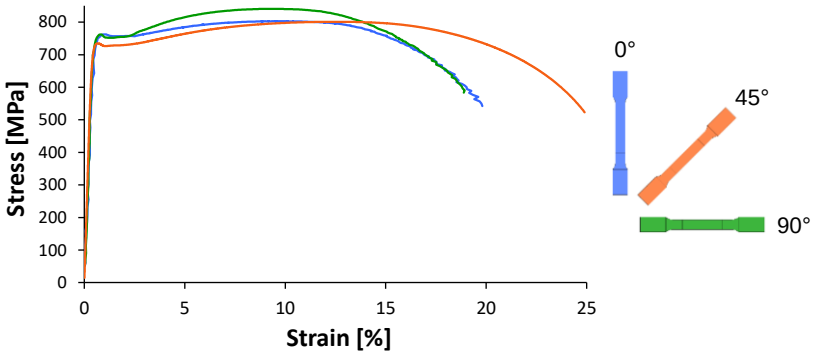

Fig. 1: Experimental engineering stress-strain curves in longitudinal, diagonal and transversal direction.

4 Parametrization based on Engineering Stress-Strain Curves

In this chapter the used LS-DYNA model, the inverse parametrization based on stress-strain curves and the verification based on local strain data from tensile and hole expansion test [9] are explained.

4.1 FE-Model Structure

All specimens are modelled with LS-DYNA with eight under-integrated constant stress solid elements (elform 1) across the thickness. All models have an identical structure as shown in Fig. 2. On all surfaces and also in the middle plane, a shell layer (elform 2) is added which uses the same nodes as the solids. These membranes are extreme thin. They do not cause an effect on the forming behavior. Thus, they allowed a direct strain analysis in the sheet plane. In the following, the strain data is taken from shells and the stress data is taken from solids.

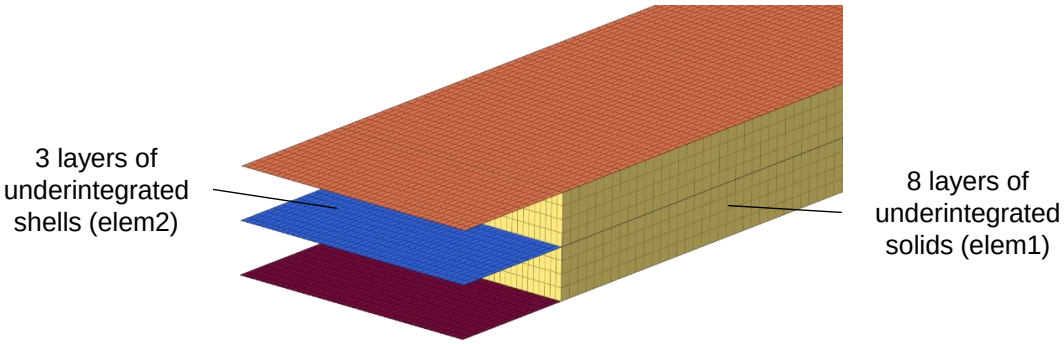

Fig. 2: Design of all modelled specimen.

4.2 Inverse Parametrization of Hardening Behavior

***MAT_TABULATED_JOHNSON_COOK_ORTHO_PLASTICITY** is used for the solid elements and has a Hill-based yield loci [2, 3]. No explicit hardening curves for compression are available, the hardening curves for tension load are used for compression, too. The hardening curve in rolling direction is also taken for the thickness direction. The extrapolation of the deployed hardening curves for 0°, 45° and 90° to rolling direction are determined by an inverse optimization of a tensile test as shown in Fig. 3. The target is the minimization of the sums of error squares from the comparison of experimental and numerical stress-strain-curves.
Equation 1 shows the extrapolation approach used according to Hocket-Sherby [10]. In this case, $k_{f,0}$ is the yield stress and $k_{f,s}$ is the stress at a plastic true strain of 1. Parameter m and p are freely selectable.

$$k_f f(\varphi) = k_{f,s} - \left(k_{f,s} - k_{f,0}\right) \cdot e^{-m \cdot \varphi^p} \quad (1)$$

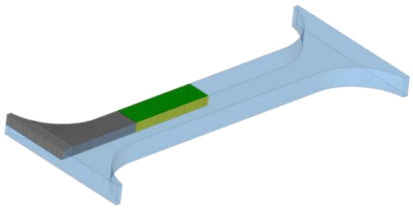

Fig. 3: Tensile test specimen modelled as 1/8 using symmetry conditions.

Fig. 4 describes the procedure of automated inverse optimization. Experimentally determined hardening curves in 0°, 45° and 90° to rolling direction are used as input data. After the extrapolation in EXCEL, the hardening curves are exported into LS-DYNA material cards and the calculations are started. The results are analyzed by a LS-PrePost script and stress-strain curves are saved. The automatically comparison with the experimentally determined stress-strain curves is done with an VBA-macro for EXCEL. Subsequently, the calculated sum of the error squares is transferred to HyperStudy. If the abort criterion is not reached, the hardening curves are automatically changed by adjusting $k_{f,s}$ and the cycle starts again.

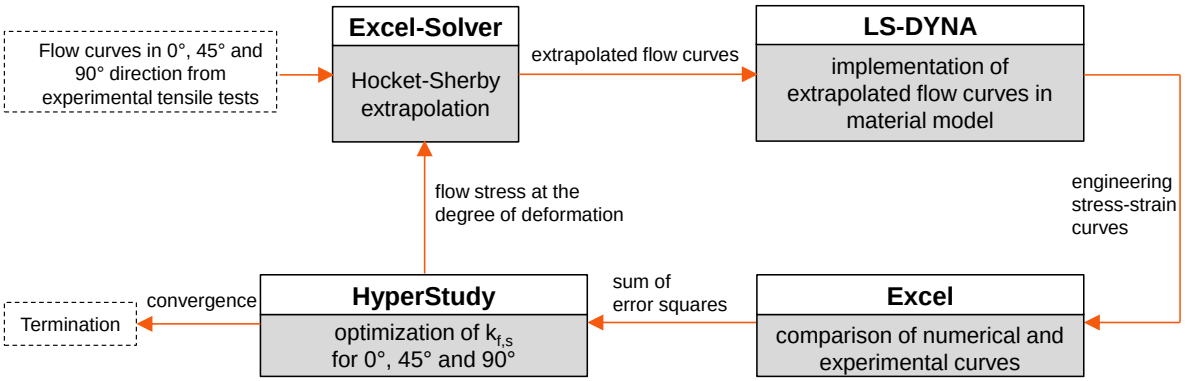

Fig. 4: Routine for inverse optimization of hardening curves.

4.3 Comparison of experimental and numerical local Strain Data from Tensile Test

The inverse parametrization aims for a good accordance of the stress-strain curves up to the beginning of localized necking. The drawback of this approach is, that the elongation is compared using a large strain gauge. As validation, after the optimization is finished, the post-necking strain concentration is compared with data from optical strain analysis system [11]. For this purpose, the slope of the major true strain is compared, which is taken centrally on the experimental specimen and the simulation specimen and is synchronized via engineering strain of the specimen. Fig. 5 shows the results for 90° to rolling direction.

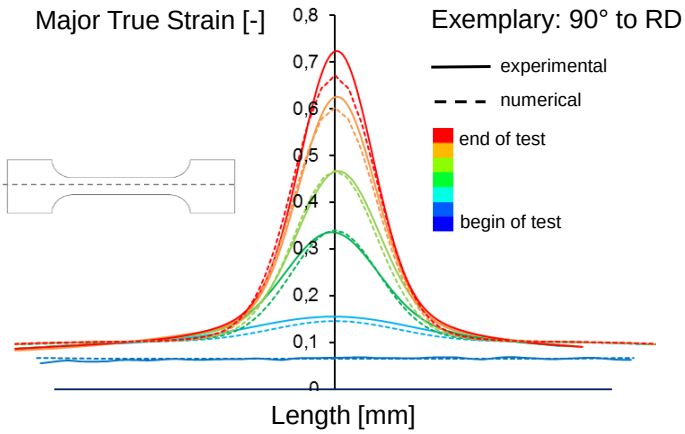

Fig. 5: Comparison of experimental and numerical local strain data from tensile test.

Deviations between simulation and experiment data increase when the necking proceeds. This is probably due to the fact that the mesh, used in the optimization routine, is not fine enough to reproduce the necking with sufficient accuracy, as larger elements have a higher stiffness.
Having a good accordance between the numerical tensile test in 0°, 45° and 90° to rolling direction to the corresponding experimental data, it has to be checked whether the interaction of the three curves shows a realistic behaviour.

4.4 Comparison of experimental and numerical local Strain Data from Hole Expansion Test with hemispherical Punch

In addition to the validation of the single hardening curves, the interaction of the three curves respectively the anisotropy is proofed by a comparison of polar diagrams showing the major true strain distribution around the hole of an experimental (solid line) and numerical (dotted line) hole expansion test with hemispherical punch. Fig. 6 shows the strain distribution of three samples, which are synchronized with the numerical experiment via the hole expansion ratio (HER). At the beginning of the hole expansion, the strain distribution is relatively circular (blue). As the test progresses, the strain distribution shows a distinct anisotropy, as the sample begins to neck at 0° and 90° to rolling direction. At 45° to rolling direction, the strain distribution is relatively good, while at 0° and 90° to rolling direction there are deviations with increasing HER. This can also be explained by the fact that the sample is not sufficiently finely meshed. Up to a certain elongation, this is sufficiently fine (45° to rolling direction) and beyond that, especially for the strong localization during necking, the mesh is too coarse.

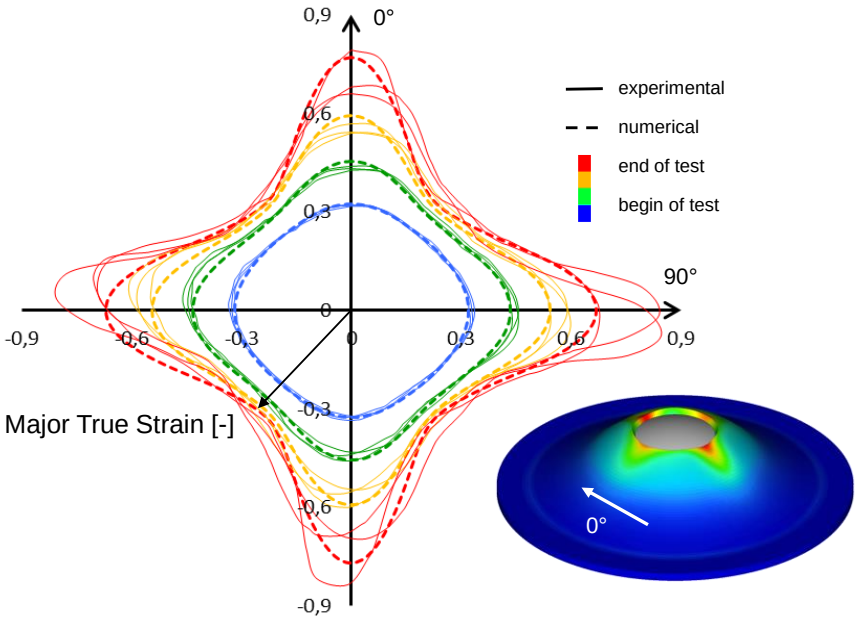

Fig. 6: Comparison of experimental and numerical local strain data from hole expansion test with hemispherical punch according to [9].

5 Experimental Determination of the True Fracture Strain from Tensile Test

The determination of the True Fracture Strain (TFS) is presently not defined in any standard. Based on the measurement of the fracture area of cracked flat tensile specimen, different evaluation methods are proposed. These methods differ mainly in whether the entire fracture surface area (TFS-A) or only individual sheet thicknesses such as the maximum thinning (TFS-T) are determined and used for the calculation.

5.1 Reduction of Area at Fracture

For evaluating the reduction of area at fracture the sample thickness is measured at three positions. As shown in Fig. 7, t_1 and t_3 are the thicknesses at the corners and t_2 is the thickness at mid-with. Assuming a parabolic shape of the edge of the fracture surface, the effective thickness t_e is calculated as

$$t_e = \frac{1}{6} * (t_1 + 4 * t_2 + t_3) \quad (2)$$

Determining the projected fracture surface width w_f at mid-thickness, the projected fracture surface area A_f is given by

$$A_f = w_f * t_e = w_f * \frac{1}{6} * (t_1 + 4 * t_2 + t_3) \quad (3)$$

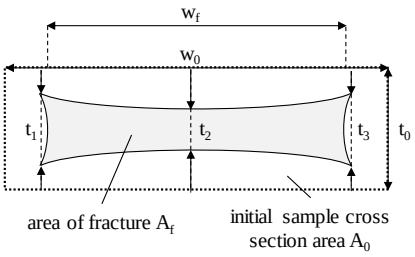

Fig. 7: Test specimen cross-sectional area of the initial sample (dotted line) and after fracture (solid line) and positions for determination of thickness and width following [4, 8].

The reduction of the cross-sectional area at fracture is defined as

$$q = \left(\frac{A_0 - A_f}{A_0}\right) \quad (4)$$

where A_0 is the cross-sectional area before testing.
The reduction of area can be converted assuming volume constancy to a “zero-gauge length elongation” value e_0. It represents the elongation in tensile direction based on infinitesimal gauge length near the fracture as [4]

$$e_0 = \frac{q}{(1-q)} \quad (5)$$

Finally, the so-called true fracture strain (TFS) at quasi zero-gauge length is defined as

$$\text{TFS-A} = \ln(1 + e_0) \quad (6)$$

5.2 Thinning of Sample Cross Section Area at Fracture

For calculating the maximum thinning of the sample cross section area at fracture, the smallest sheet thickness t_f within the fracture surface is determined. The absolute thickness strain e_f is given as the ratio between the reduction of thickness to the initial thickness t_0 [6]:

$$e_f = \frac{(t_0 - t_f)}{t_0} \quad (7)$$

Consequently, the absolute logarithmic thickness strain TFS-T is designated as

$$\text{TFS-T} = -\ln\left(\frac{t_f}{t_0}\right) \quad (8)$$

6 Parametrization based on data from TFS determination

However, the choice of specimen geometry seems to influence the TFS result. Therefore, different width/thickness ratios (w/t ratio) of the tensile specimens are considered in the numerical simulation. For a sheet thickness of 4.0 mm, the widths 4, 6, 10 and 20 mm are taken into account and in case of 2.0 mm thickness a width of 20 mm.
All numerical tensile specimens have an initial edge lengths of 0.05 x 0.1 x 01 mm (x, y, z-direction), where x-direction corresponds to the loading direction of a longitudinal tensile test. With this configuration, it is achieved, that the elements are close to the ideal cubic shape over a larger range of strain. In order to determine the TFS value, the fracture surface is realized by using a MMC (Modified Mohr-Coulomb) failure model for the selected steel [12].

6.1 Results of the numerical Investigation with Focus on Hardening Behavior

Fig. 8 (left) shows the superposition of the resulting fracture area from the numerical model in case of an initial width of 20.0 mm and thickness of 4.0 mm as well as the contours of the experimental tests. Regarding the small deviations in the thickness profile, width and maximum thickness reduction, the compromise in accuracy and computing time is regarded to be reasonable.

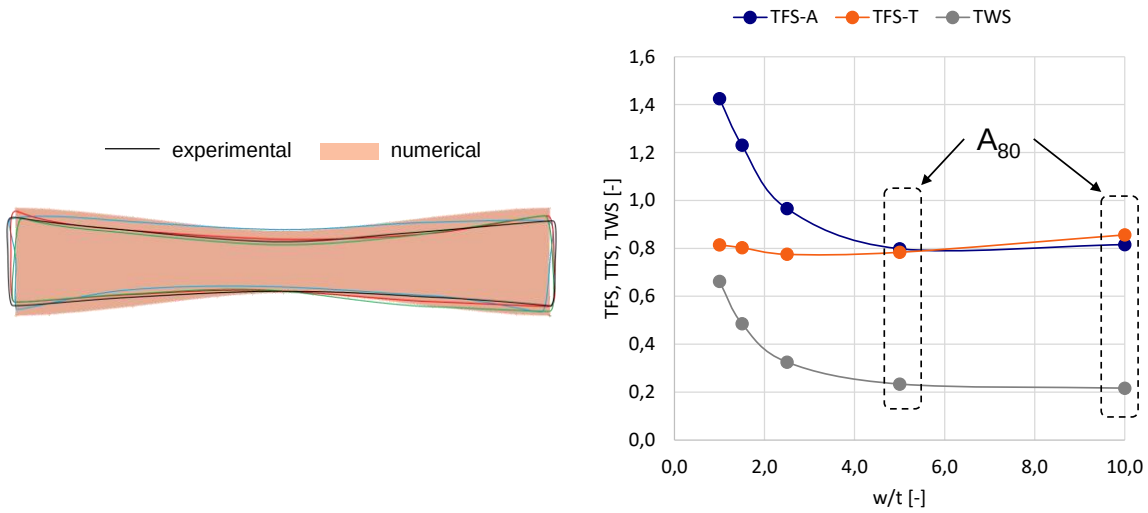

Fig. 8: Comparison of the fracture surface from virtual and experimental tests with initial width of 20.0 mm and thickness of 4.0 mm (left) and the TFS values related to w/t ratios from the virtual experiments (right).

The virtual experiments show a strong dependence of the TFS-A and the TWS value (true width strain) on the specimen geometry (Fig. 8 right) under consideration of different w/t ratios, especially at small ratios. This confirms the experimental results of Wagner [5]. The TFS-T value based on thickness reduction shows only a slight reduction with increasing w/t ratios.
The reason why the TFS-A value forms a constant plateau at w/t ratios of 5 to 10 is shown by comparing the section cuts taken instantly before cracking (solid line) with the initial rectangular section cuts (dotted line) (Fig. 9). For all tensile specimen shapes, a similar thickness reduction occurs in the middle of the specimen due to necking under plane strain condition. With increasing w/t ratios, the material flow from the width is prevented geometrically. This is resulting in a decreasing TWS value, which has a direct influence on the TFS-A value (Fig. 8).

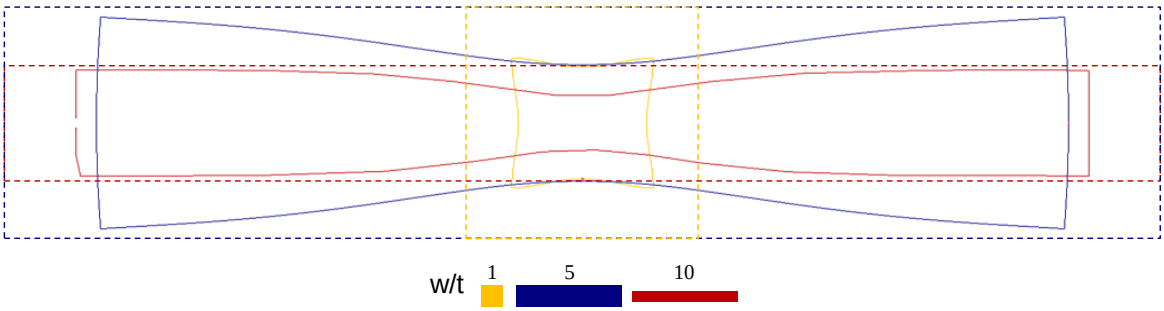

Fig. 9: Comparison of section cuts of virtual tensile specimens in initial condition (dotted line) and shortly before cracking (solid line).

6.2 Results of the numerical Investigation with Focus on Failure Behavior

Fig. 10 shows the comparison of the stress states of the considered w/t ratios. The Lode angle parameter is plotted over the triaxiality for the elements which failed in the virtual tensile test. The lode angle parameter is required for the usage of damage modelling in the 3D application [12]. At a value of 1 it describes a tensile load, at 0 shear load and at -1 compression load. As expected, at the beginning of the necking (Fig. 10 left) all specimen shapes are subjected to uniaxial tension. In case of specimens

with large w/t ratios, it changes into a shear load during necking (Fig. 10 right). This confirms the experimental results of Wagner [5].

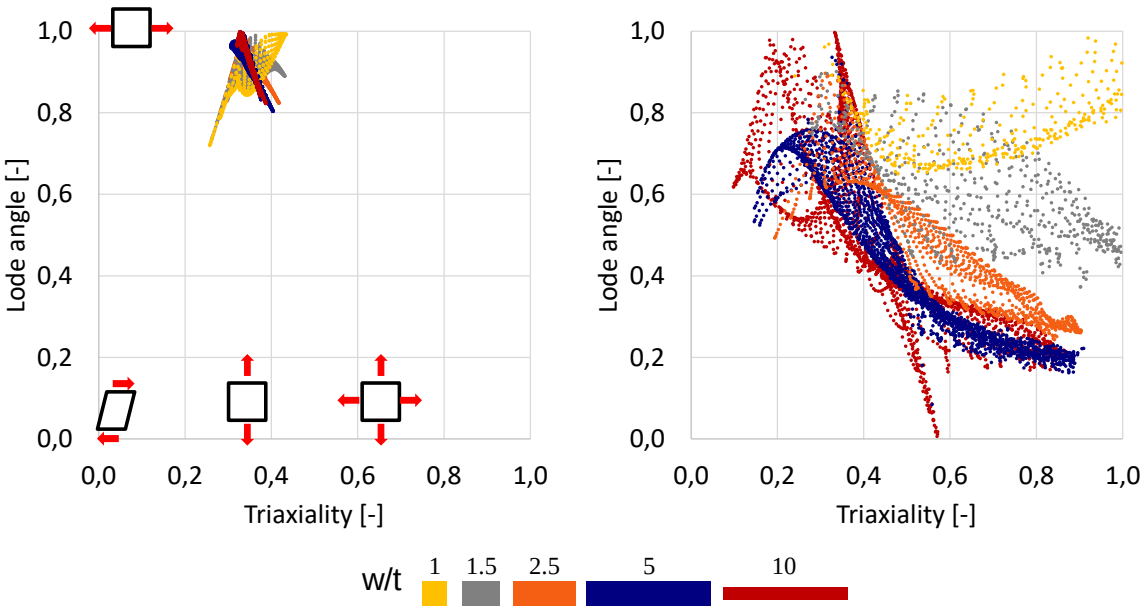

Fig. 10: Lode angle parameter related to triaxiality of the elements which failed for both at the beginning of necking (left) and the end of necking (right).

Beyond a critical w/t ratio, the shear load increases to such an extent that the fracture behavior changes from cup and cone type of fracture to shear type of fracture. The consideration of a further increase of the w/t ratio leads to the expected shear fracture in the virtual tensile tests (Fig. 11).

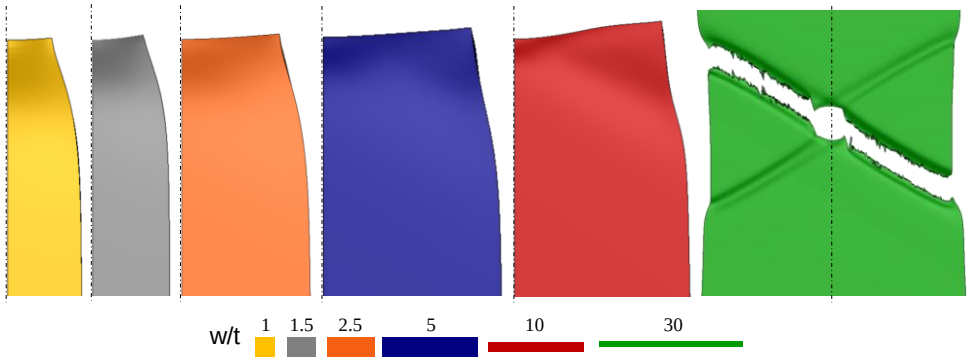

Fig. 11: Influence of w/t ratios on development of fracture type (from cup cone to shear) using 1/4 tensile specimen due to high computing time. In case of w/t = 20 the complete specimen is used for simulation

7 Summary and Conclusion

The inverse optimization of the three stress-strain-curve extrapolations seems to be a practical way to fit ***MAT_TABULATED_JOHNSON_COOK_ORTHO_PLASTICITY**. The comparison of experimental and numerical strain data shows a good accordance over a wide range of strain.
The comparison of the numerical and experimental major strain on a section cut along the tensile specimens allows a comparison of strains with a much smaller strain gauge. This leads to a better understanding of the strain distribution in the zone of localized necking and causes no additional optimization time.
The optimization of the interaction of the three hardening curves can be achieved by a comparison with the strain data from a hole expansion test with a hemispherical punch.

The comparison of local strain data from an optical strain measurement system could be easily adopted to the optimization framework. An additionally inclusion of a numerical hole expansion test would increase the calculation time too much.
The massive amount of calculation time avoids also the use of TFS in an optimization. Due to the very fine mesh, each optimization cycle would take about a day. However, the contour of the fracture surface is a very useful target for the fine adjustment of hardening.
Due to influence of the width to thickness ratio of a tensile specimen on the stress state, a simple experimental variation of this ratio indicates the changeover from ductile to shear fracture. With the knowledge of corresponding w/t ration, a fracture criterion could be adjusted.

8 Literature

[1] Schneider M., Teschner M. and Westhäuser S.: “Analysis of stress states during experimental determination of cut-edge formability”, LS-DYNA Anwenderforum, 2018.
[2] Haigh S. H.: “An anisotropic and asymmetric Material Model for Simulation of Metals under dynamic Loading”, Ph.D. Thesis, 2016.
[3] Haight S., Kan C.-D. and Du Bois P.: “Development of a Fully- Tabulated, Anisotropic and Asymmetric Material Model for LS-Dyna (*MAT_264)”, European LS-Dyna Conference, 2015.
[4] Hance B.: “Advanced High Strength Steel: Deciphering Local and Global Formability”, International Automotive Body Congress, 2016.
[5] Wagner, L. and Larour, P.: “Influence of specimen geometry on measures of local fracture strain obtained from uniaxial tensile tests of AHSS sheets”, IOP Conference Series: Materials Science and Engineering, 2018, 418, 12074, https://DOI.org/10.1088/1757-899X/418/1/012074.
[6] Larour, P., Freudenthaler, J. and Weissböck, T.: “Reduction of cross section area at fracture in tensile test.Measurement and applications for flat sheet steels”, J. Phys.: Conf. Ser., 2017, 896, 12073, https://DOI.org/10.1088/1742-6596/896/1/012073.
[7] Westhäuser S., Schneider M. and Denks I. A.: “Local Ductility and Edge Crack Resistivity of Advanced High Strength Steel Grades”, International Conference on „New Developments in Sheet Metal Forming”, 2018.
[8] Denks, I. A., Schneider, M. and Westhäuser, S.: “On the relation of global and local ductility to edge crack resistivity of advanced high strength steel sheets”, Steel Research International, 2019, https://DOI.org/10.1002/srin.201800460.
[9] Schneider M., Peshekhodov I., Bouguecha A. and Behrens B.-A.: “A new approach for user-independent determination of formability of a steel sheet sheared edge”, Prod. Eng. Res. Devel., 2016, https://DOI.org/10.1007/s11740-016-0677-4.
[10] Hockett, J. E. and Sherby, O. D.: “Large strain deformation of polycrystalline metals at low homologous temperatures”, Journal of the Mechanics and Physics of Solids, 1975, 87–98, https://DOI.org/10.1016/0022-5096(75)90018-6.
[11] Westhäuser S., Schneider M. and Denks I. A.: “On the Relation of Local Formability and Edge Crack Sensitivity”, International Conference on Steels in Cars and Trucks, 2017.
[12] Bai, Y. and Wierzbicki, T.: “A new model of metal plasticity and fracture with pressure and Lode dependence”, International Journal of Plasticity, 2008, 24, 1071–1096, https://DOI.org/10.1016/j.ijplas.2007.09.004.